# Annexin A1 regulates TGF-β signaling and promotes metastasis formation of basal-like breast cancer cells

Marjo de Graauw[a,1], Martine H. van Miltenburg[a,1], Marjanka K. Schmidt[b], Chantal Pont[a], Reshma Lalai[a], Joelle Kartopawiro[a], Evangelia Pardali[c], Sylvia E. Le Dévédec[a], Vincent T. Smit[d], Annemieke van der Wal[d], Laura J. Van't Veer[b], Anne-Marie Cleton-Jansen[d], Peter ten Dijke[c], and Bob van de Water[a,2]

[a]Division of Toxicology, Leiden/Amsterdam Center for Drug Research, Leiden University, 2300 RA, Leiden, The Netherlands; [b]Department of Pathology, Netherlands Cancer Institute-Antoni van Leeuwenhoek Hospital, 1066 CX, Amsterdam, The Netherlands; [c]Department of Molecular Cell Biology and Centre for Biomedical Genetics, Leiden University Medical Center, 2300 RA, Leiden, The Netherlands; and [d]Department of Pathology, Leiden University Medical Center, 2300 RC, Leiden, The Netherlands

Annexin A1 (AnxA1) is a candidate regulator of the epithelial- to mesenchymal (EMT)-like phenotypic switch, a pivotal event in breast cancer progression. We show here that AnxA1 expression is associated with a highly invasive basal-like breast cancer subtype both in a panel of human breast cancer cell lines as in breast cancer patients and that AnxA1 is functionally related to breast cancer progression. AnxA1 knockdown in invasive basal-like breast cancer cells reduced the number of spontaneous lung metastasis, whereas additional expression of AnxA1 enhanced metastatic spread. AnxA1 promotes metastasis formation by enhancing TGFβ/Smad signaling and actin reorganization, which facilitates an EMT-like switch, thereby allowing efficient cell migration and invasion of metastatic breast cancer cells.

Annexin A1 (AnxA1) belongs to the family of calcium/phospholipid-binding and actin regulatory proteins (1). Using proteomic analysis we have previously identified AnxA1 and its family member AnxA2 as candidate regulators of oncogene-induced cell morphology switch (2). During such a switch, tumor cells change from an epithelial- to a more migratory, mesenchymal-like phenotype. This switch enables them to increase their motility and invasiveness, allowing metastasis and progression of breast cancer (3). Despite the identification of AnxA1 as one of several cellular proteins that is differentially expressed during the progression of tumors to more malignant states (4), a functional role for AnxA1 in breast cancer progression and metastasis is lacking (5, 6). Therefore, we set out to study AnxA1 expression in different breast cancer cell subtypes and its role and mechanism in the control of breast cancer progression and metastasis formation.

Several different subtypes of breast carcinomas can be identified based on gene expression profiling studies (e.g., luminal A, luminal B, normal breast-like, ErbB2-positive, and basal-like) (7, 8). These subtypes differ in their morphology, clinical course, and response to therapy. For example, whereas the luminal subtype is characterized by its mild invasive capacity and relatively good clinical outcome, the basal-like subtype is characterized by enhanced invasiveness and formation of distant metastasis and, thereby, a poor clinical outcome (7, 9). The enhanced metastatic capacity of basal-like breast cancer (BLBC) is associated with their migratory, mesenchymal-like phenotype (10).

Here, we show that high AnxA1 expression is associated with the BLBC subtype in a panel of breast cancer cell lines. Depletion of AnxA1 in BLBC cells resulted in reversal of their migratory, mesenchymal-like phenotype, which was associated with actin reorganization, decreased TGFβ/Smad signaling, and a reduction in the number of spontaneous lung metastasis in vivo. Moreover, using tissue microarrays (TMAs), we show that AnxA1 clearly discriminates BLBC patients from other breast cancer patients.

## Results

### High AnxA1 Expression in BLBC Is Associated with Their Mesenchymal-Like Phenotype.
To establish the relationship between AnxA1 expression and breast cancer cell phenotype, a panel of human breast cancer cell lines was screened for AnxA1 expression. AnxA1 was highly expressed in cells that were characterized as mesenchymal-like (11) and classified as cytokeratin (CK)5$^+$/estrogen receptor (ER)$^-$ BLBC cells (12, 13) (Fig. 1 A and B). In contrast, CK5$^-$/ER$^+$ luminal-like breast cancer cells almost completely lacked AnxA1 (Fig. 1 A and B).

To verify whether AnxA1 regulates the migratory, mesenchymal-like phenotype of BLBC cells, AnxA1 was depleted in a selection of these cells by using either transient siRNA- or stable lentiviral shRNA-mediated knockdown. In control cells, AnxA1 is localized at the plasma membrane site, in the actin-rich membrane ruffles (MDA-MB-231), and migratory tips (4T1), which are required for migration, invasion, and metastasis (Fig. 1 C–E). In all selected BLBC cells, AnxA1 knockdown resulted in a morphological switch from a migratory, mesenchymal-like phenotype to a resting, epithelium-like phenotype (Fig. 1 C–E and Fig. S1 A–D). This reversal of the migratory phenotype was associated with a clear rearrangement of the actin cytoskeletal network; actin-rich ruffles were lost and long F-actin stress fibers were obtained (Fig. 1 D and E). Moreover, AnxA1 knockdown induced the formation of β-catenin-containing cell-cell junctions in all cells, which were most clearly visible in the highly motile MTLn3 cells (Fig. S1 C and D). In addition, AnxA1 knockdown significantly reduced the migration distance and random cell migration speed of siAnxA1 MTLn3 cells (Fig. S1 E–G and Movies S1, S2, and S3). The AnxA1 knockdown-induced epithelium-like morphology of MTLn3 cells was rescued by ectopic expression of AnxA1 (Fig. S1 C and D). These combined data demonstrate that AnxA1 is involved in an EMT-like switch, facilitating cell migration in vitro.

### Knockdown of AnxA1 in BLBC Cells Impairs TGF Signaling.
The switch from an epithelial to a mesenchymal-like phenotype is, among other pathways, regulated by TGFβ signaling (14). Because AnxA1 knockdown induces a morphological switch from a mesenchymal- to an epithelium-like phenotype in different BLBC cells, we determined its influence on TGFβ signaling. TGFβ induces clustering of TGFβRI and II and, subsequently, phosphorylation of Smad2. AnxA1 knockdown in MDA-MB-231 cells impaired Smad2 phosphorylation in response to TGFβ exposure (Fig. 2 A and B). Smad2 phosphorylation is a trigger for Smad2 to form a complex with Smad4,
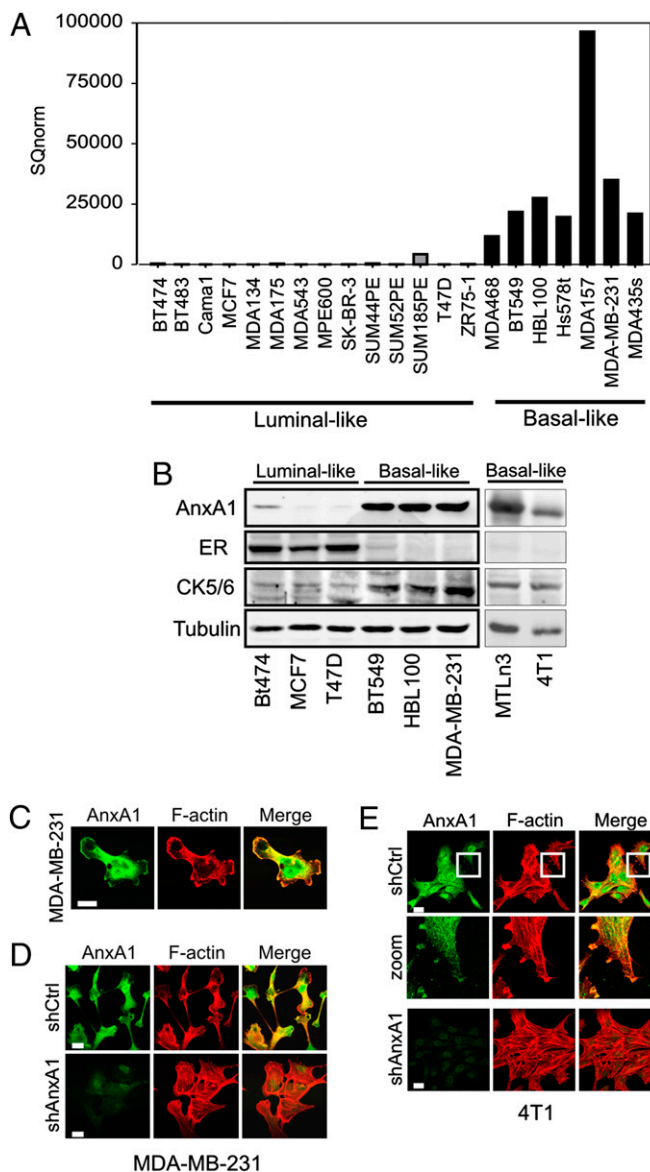
**Fig. 1.** AnxA1 expression in BLBC is associated with their migratory pheno-
type. (*A*) A panel of human breast cancer cell lines was analyzed for AnxA1
mRNA levels. (*B*) Western blot analysis of AnxA1 protein levels in luminal-like
(BT474, MCF7, T47D) versus basal-like (HBL100, BT549, MDA-MB-231)
human breast cancer cell lines and basal-like mouse 4T1 and rat MTLn3 cells. (*C*) AnxA1
localization was determined in MDA-MB-231 cells by staining for AnxA1
(green) and actin (red). (*D* and *E*) Knockdown in MDA-MB-231 (*D*) and 4T1 cells
(*E*) was established by using lenti-viral shRNA specific for turbo-GFP (Control
shRNA) and AnxA1 (AnxA1 shRNA1). Cells were plated on collagen and sub-
sequently fixed and stained for AnxA1 and F-actin (rhodamin-phalloidin).
(Scale bars: 20 μm.) Data are representative of three independent experiments.

resulting in nuclear translocation of the Smad2/Smad4 complex and
subsequent gene transcription. AnxA1 knockdown MDA-MB-231
cells exposed to TGF show less nuclear translocation of Smad4 (Fig. 2
*C* and *D*). In addition, knockdown of AnxA1 in MDA-MB-231,
BT549, and MTLn3 cells resulted in reduced activity of TGFβ/
Smad3/Smad4-driven (CAGA)$_{12}$-luciferase transcriptional reporter
activity (Fig. 2 *E–G*), indicating that AnxA1 is also involved in the
regulation of TGFβ/Smad3 response. Furthermore, the TGFβ-type I
receptor inhibitor SB-431542 (15) reduced (CAGA)$_{12}$-luciferase
activity in MTLn3 cells both in the absence and presence of TGFβ
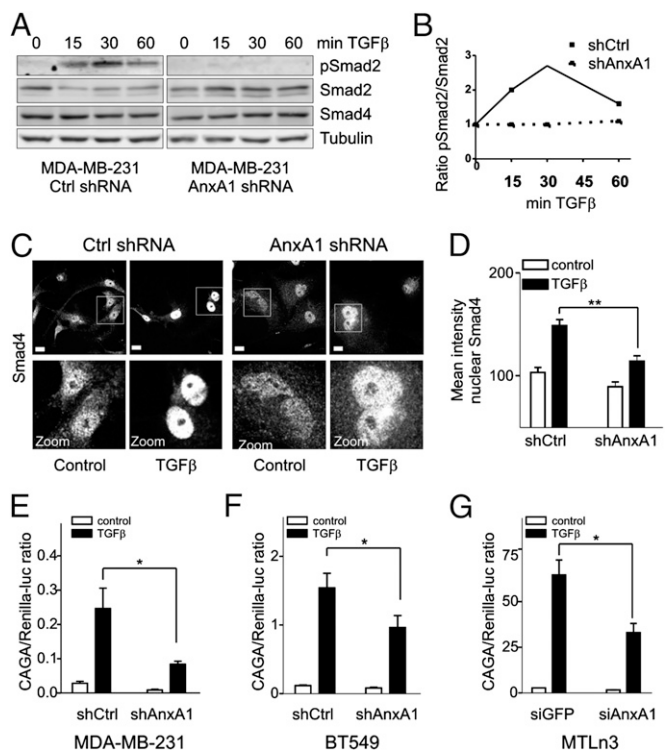(Fig. S2*A*), and reversed the mesenchymal-like phenotype (Fig. S2*B*)



**Fig. 2.** Knockdown of AnxA1 in BLBC cells impairs TGF signaling. (*A*) Stable
MDA-MB-231 knock-down cells were exposed to TGFβ1 (0.5 ng/mL) for indicated
time periods. Phosphorylation of Smad2, Smad2 and Smad4 expression was
determined by Western blotting. (*B*) Quantification of Smad2 phosphorylation.
Translocation of Smad4 was determined by Smad4 staining of MDA-MB-231 cells
exposed to TGFβ1 for 30 min (*C*) and quantification of nuclear intensity (*D*).
TGFβ1-induced transcription was determined by transient transfection of
(CAGA)$_{12}$-luciferase in AnxA1 depleted MDA-MB-231 (*E*), BT549 (*F*), and MTLn3
cells (*G*). After transfection, cells were exposed to TGFβ1 (0.5 ng/mL) for 24 h.

similar to the morphological switch observed in AnxA1 knockdown
cells (Fig. S1 *C* and *D*). Moreover, TGFβ alone enhanced cell scat-
tering (Fig. S2*B*). Altogether, the data suggest that AnxA1 is involved
in TGFβ-induced EMT-like switch.

**Expression of AnxA1 Induces an EMT-Like Switch by Activation of the
TGFβ Pathway.** Next, we considered whether AnxA1 expression in
a typical luminal-like breast cancer cell line that has low AnxA1
expression, would induce a scattered phenotype. Indeed, AnxA1
expression in luminal-like MCF7 cells resulted in increased cell
scattering (Fig. 3 *A* and *B*), which was associated with a disruption
of F-actin stress fibers, an increase in actin-rich ruffles, and a
decrease in β-catenin-containing cell-cell junctions (Fig. 3 *A* and *B*
and Fig. S2*E*). MCF7 cells expressing AnxA1 showed increased
TGFβ-induced Smad3/Smad4 transcriptional reporter activity,
explaining the increase in cell scattering (Fig. 3*C*). Increased
TGFβ-induced Smad3/Smad4 transcriptional reporter activity was
also observed in epithelium-like cell lines BT474 and T47D cells
(Fig. S2 *C* and *D*, respectively) The AnxA1-induced increase in
Smad3/Smad4 transcriptional response was inhibited by the TGFβ
type I receptor inhibitor SB-431542, suggesting that AnxA1 might
affect an autocrine signaling loop of TGFβ–induced receptor
activation (Fig. 3*C*). This notion was supported by the observation
that AnxA1-expressing MCF7 cells exposed to the SB-431542
showed a morphological change from a mesenchymal-like to an
epithelial phenotype (Fig. 3 *D* and *E*). Overall, our data strongly
support the importance of AnxA1 in the regulation of a morpho-
logical switch from a resting epithelium-like to a migratory phe-
notype through regulation of the TGFβ/Smad pathway.
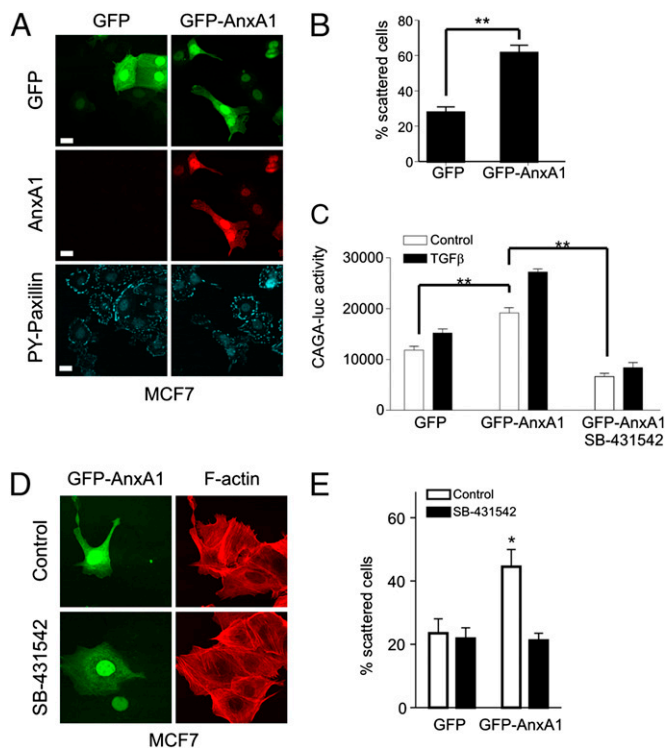
CELL BIOLOGY

**Fig. 3.** AnxA1 induced cell scattering in luminal-like MCF7 cells through TGFβ pathway activation. (*A*) MCF7 cells were transfected with GFP or GFP-AnxA1. Cells were plated on collagen for 24 h and subsequently fixed and stained for AnxA1. Cells were costained with phosphoY118-paxillin to visualize all cells within the frame. (*B*) The number of scattered cells was determined for the GFP positive cells. (*C*) Cotransfection of (CAGA)$_{12}$-luc and GFP-AnxA1 was performed and cells were exposed to TGFβ and/or SB-431542 and, thereafter, luciferase activity was measured. (*D*) MCF7 cells expressing GFP-AnxA1 were exposed to SB-431542 and stained for F-actin. (*E*) Cell scattering induced by AnxA1 expression was reduced by SB-431542. (Scale bars: 20 μm.) Data are representative of three independent experiments. *, $P < 0.05$; **, $P < 0.01$.

**Knockdown of AnxA1 Decreases the Metastatic Potential of Highly Aggressive 4T1 Cells.** Next, we determined whether AnxA1 depletion from highly invasive breast cancer cells can reduce metastasis formation in vivo. Therefore, the well characterized invasive breast cancer cell line 4T1 was used, which is able to spontaneously metastasize from a primary tumor in vivo (16). To establish AnxA1 depletion in 4T1 cells, two independent lenti-viral shRNA were used (Fig. 4*A*). The control cell line expresses a shRNA sequence against turbo-GFP. Cells were injected into the mammary fat pads of 12-week-old Rag2$^{-/-}$/γc$^{-/-}$ mice. Knockdown of AnxA1 had no effect on primary tumor growth (Fig. 4*B* and Fig. S3*B*). Mice were killed at day 22, and histological evaluation of the primary tumor confirmed decreased expression of AnxA1 in tumors derived from AnxA1 shRNA cells (Fig. S3*A*). Lungs of animals injected with control 4T1 contained >130 surface metastases (Fig. 4 *C–E*), whereas animals injected with either AnxA1 knockdown 4T1 contained on average ≈30 surface metastases (Fig. 4 *C–E*). In line with our findings in Rag2$^{-/-}$/γc$^{-/-}$ mice, AnxA1 knockdown did not affect primary tumor growth, but significantly reduced the number of lung metastases in syngenic Balb/C mice (Fig. S3 *B* and *C*). In addition, metastasis formation of AnxA1 knockdown MTLn3 cells was markedly reduced (Fig. S3 *D* and *E*).

The reduction in metastasis formation by AnxA1 depletion was associated with reduced TGFβ/Smad signaling. Smad2 phosphorylation in primary tumors was reduced as well as the nuclear levels of Smad4 (Fig. 4 *F* and *G*, respectively). Our in vivo data
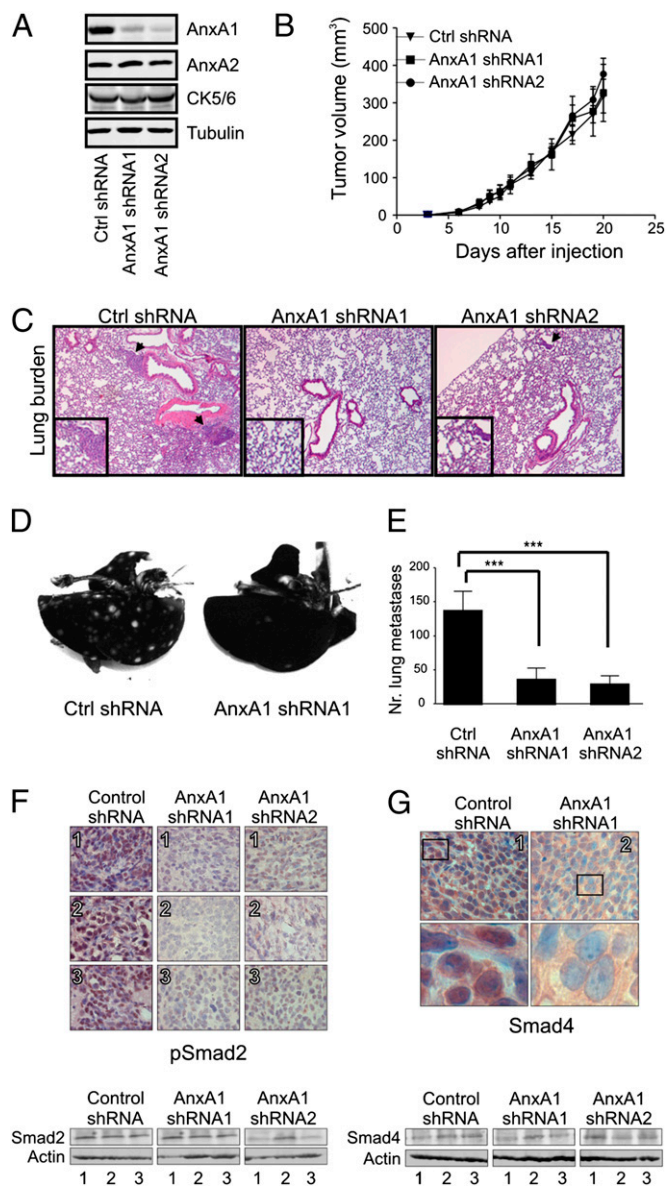


**Fig. 4.** Knockdown of AnxA1 decreases the metastatic potential of highly invasive 4T1 cells via decreased TGFβ signaling. (*A*) Mouse breast cancer 4T1 cells were transduced with lenti-viral shRNA specific for turbo-GFP (control shRNA) and two sequences for AnxA1 (AnxA1 shRNA1 and 2). AnxA1 knockdown was determined by Western blot analysis. (*B*) AnxA2 levels were included in the analysis to show specificity of the shRNAs. Equal loading was confirmed by tubulin staining. AnxA1 shRNA1 (*n* = 6), AnxA1 shRNA2 (*n* = 6), and control shRNA (*n* = 7) 4T1 cells were injected into the mammary fat pad of 12-week-old Rag2 $^{-/-}$ /γc $^{-/-}$ mice. Tumor volume was determined as described in *Materials and Methods*. (*C*) At 22 days after injection, the mice were killed and lungs were isolated. Lung sections were stained for H&E to visualize lung metastases. Lungs were inoculated with ink as described under *Materials and Methods* (*D*) and surface metastases were quantified (*E*). ***, $P < 0.001$. Primary tumors were stained for p-Smad2 and Smad4 using Nova-Red staining and quantified for equal expression of Smad2 (*F*) and Smad4 (*G*) by using Western blotting. * $P < 0.05$, ** $P < 0.01$.

indicate that the morphological changes induced by AnxA1 knockdown are linked to a decrease in breast cancer progression via the effect on TGFβ/Smad signaling.

**AnxA1 Distinguishes Basal-Like Breast Cancer Patients from Others.** To verify our finding that AnxA1 is expressed in a specific subset of breast cancer cells, human TMA containing tissues of 452 breast
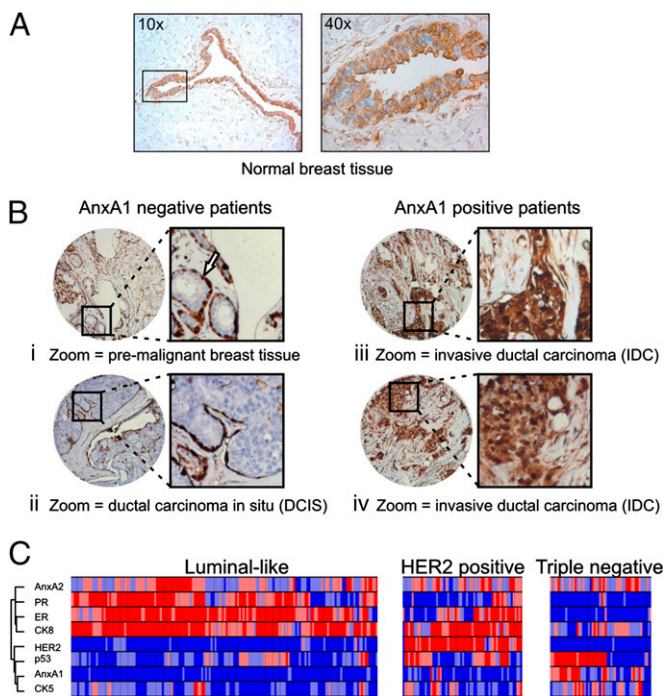
**Fig. 5.** AnxA1 discriminates BLBCs from other subtypes. (*A*) Normal breast tissue was stained for AnxA1. (*B*) Human breast cancer tissues (TMA of 452 patients) were screened for AnxA1, AnxA2, and six clinical markers CK5, CK8, ER, PR, HER2, and p53. Representative images are shown for pre-malignant breast tissue (*a*; note the AnxA1 positive myoepithelial cells pointed by an arrow), AnxA1 negative ductal carcinoma in situ (DCIS) (*b*), and AnxA1 positive, invasive ductal carcinoma (IDC) (*c* and *d*). Only those breast carcinomas where staining for all of the eight immunohistochemical markers was successful (n = 295) were included for hierarchical unsupervised cluster analysis (*B*) and tumors were divided luminal-like, HER2+, and triple negative groups (*C*).

cancer patients were analyzed. In contrast to normal breast tissue where AnxA1 is localized in both the luminal and myoepithelial cell layer (Fig. 5*A*), in premalignant breast tissue, AnxA1 was mainly expressed in the myoepithelial cell layer, where it localized both in the cytosol as well as the nucleus (Fig. 5*Ba*). In breast cancers, the majority of the tumor tissue showed negative (Fig. 5*B a* and *b*; n = 323) or low expression (n = 85) of AnxA1, whereas ≈10% showed high expression of AnxA1 (Fig. 5*B c* and *d*; n = 44). The AnxA1-negative/low cases included both ductal carcinoma in situ (DCIS) as well as invasive ductal carcinoma (IDC), whereas AnxA1-positive tumors included mainly IDC (Fig. 5*B* and Fig. S4). Further analysis revealed that AnxA1 expression correlated with high pathologic tumor grade (*P* < 0.001; Fig. S5*A* and Table S1).

In addition to AnxA1, TMAs were stained and scored for AnxA2 and six markers currently used for the identification of specific subgroups of breast tumors [e.g., human epidermal growth factor receptor 2 (HER2), the hormonal receptors ER and PR (progesterone receptor), basal and luminal CK5 and CK8, respectively, and p53]. Statistical analysis of the expression data confirmed an overall significant correlation between AnxA1 expression and proteins associated with BLBC (e.g., p53[high], CK5^{high}, ER[low], CK8^{low}) (Fig. S5 *B–E* and Tables S2, S3, S4, and S5), suggesting that AnxA1 is also predictive for BLBC in breast cancer patients.

Unsupervised hierarchical clustering of the protein expression data subdivided all breast cancers into four clusters: a small undefined CK5^{+}/8[+]/ER[+] group (1; ≈5%), ER[+]/luminal-like (2; ≈60%), HER2-positive (3; ≈20%), and triple negative (ER[−]/PR[−]/HER2^{−}) (4; ≈15%) (Fig. 5*C* and Fig. S5). AnxA1 was almost exclusively expressed in the small CK5^{+}/8[+]/ER[+] sub-group (1) and triple negative breast cancer subgroup (4), whereas its close family member AnxA2 was expressed in all four clusters. Moreover, a clear correlation was found between p53 and AnxA1 expression within the triple negative subgroup. Although, triple negative breast cancers are described as a het-erogeneous group of cancers, the majority display a basal-like phenotype (17). CK5 expression, either in association with the lack of ER/PR/HER2 or alone (17, 18), is often used to define the poor prognosis BLBC subtype. Our cluster analysis revealed that AnxA1 clusters directly with CK5, a marker for the BLBC subtype (Fig. 5*C*). Moreover, our unsupervised hierarchical clustering showed that CK5 is not solely expressed in the triple negative group, but also in the luminal-like and HER2^{+} tumor samples. In contrast, AnxA1 is almost exclusively expressed in the triple negative subgroup [marker prediction of a tumor to be in the triple negative subgroup versus any other subgroup (Odd Ratios; 95% confidence interval)]: CK5 2.2 (1.2–4.2), *P* = 0.01, and AnxA1 10.5 (4.9–22.2), *P* < 0.0001. Because of the small number of AnxA1-positive patients, we were unable to sig-nificantly correlate AnxA1 protein expression to recurrence and relapse-free survival, yet a clear trend was observed between AnxA1 protein expression and recurrence. In addition, within the specific gene signature for poor prognosis defined by van de Vijver et al. (19), AnxA1 gene expression was significantly higher in basal-like than in the other tumor subtypes (*P* < 0.001; Table S6). Altogether our data shows that AnxA1 is associated with the BLBC subtype and functionally involved in BLBC progression and metastasis formation by regulating TGFβ-signaling and actin cytoskeletal reorganization.

## Discussion

BLBCs represent <10% of all breast cancers and show enhanced invasiveness and metastatic potential (9). Given the poor disease prognosis associated with BLBC, improving methods to accu-rately identify BLBC in the clinic as well as better mechanistic understanding of the molecular programs that define the meta-static potential are essential. Our data demonstrated that BLBCs express high levels of AnxA1 and that AnxA1 is important for their capacity to metastasize because it facilitates a migra-tory phenotype.

Depletion of AnxA1 in a panel of BLBC cells resulted in reversal of their migratory phenotype and inhibition of lung metastasis formation. We show that AnxA1 expression controls the aggressive behavior of BLBC cells via a TGFβ-mediated EMT-like switch, thereby allowing a migratory phenotype of breast cancer cells and metastasis formation. AnxA1 knockdown sup-pressed TGFβ-induced Smad2 phosphorylation, Smad4 nuclear translocation and Smad3/Smad4-driven transcriptional reporter activity. Moreover, primary tumors with AnxA1 knockdown had a reduced Smad2 phosphorylation and Smad4 nuclear localization. A biological role of AnxA1 is not restricted to BLBC-like tumor cells. Despite the fact that luminal-like breast tumor cells do not express AnxA1, ectopic expression of AnxA1 in luminal-like MCF7 cells resulted in a clear EMT-like switch. Moreover, enhanced TGFβ signaling now occurred in these cells. Therefore, it is likely that such a role of AnxA1 is also relevant in other aggressive tumor cell types. Our data on the role of TGFβ in the metastasis formation are in conjunction with the study of Deckers et al. (20) that demonstrated that TGFβ signaling via Smad4 is required for TGFβ-induced EMT and bone metastasis formation of NMuMG and MDA-MB-231 cells respectively. Moreover, TGFβ in the breast tumor microenvironment was shown to prime cancer cells for metastasis to the lungs (21), and TGFβ antagonists reverse the migratory phenotype that is characteristic of BLBC cells, thereby affecting the progression of BLBC (22). We antici-pate that AnxA1 is a central player in TGFβ-signaling dependent cancer progression.

Members of the annexin family have been shown to be involved in endocytosis (23–27). Although AnxA1 was enriched in membrane fractions containing early endosomes (28), it remains unclear how AnxA1 is involved in endocytosis and, in particular, endocytosis of TGFβ-receptors. Inhibition of TGFβ receptor endocytosis results in decreased Smad2 phosphorylation and Smad-mediated gene transcription (29–31). We propose that AnxA1 may influence TGFβ signaling by interfering with TGFβ-receptor endocytosis.

In addition to its direct effect on endocytosis, AnxA1 may influence internalization of TGFβ receptors indirectly via regulation of the actin cytoskeleton like has been described for AnxA2 (27). Decreased actin cytoskeletal dynamics as observed in our AnxA1 knockdown cells might stiffen the cell membrane, thereby impeding TGFβ-receptor internalization. Compared with other actin-regulatory proteins, AnxA1 has the unique property to bind both phospholipids at the plasma membrane and F-actin, thereby stabilizing and/or regulating membrane–actin interactions (32).

To define BLBCs in the clinic, pathologists often use immunohistochemical staining of the classical marker CK5. However, we and others show that CK5 is also expressed in luminal-like and HER2 breast cancers, suggesting that the sole reliance on CK5 could result in false-positive characterization (Fig. 5) (33). Our TMA data analysis revealed a significant correlation between high AnxA1 protein expression and the BLBC subtype without any high expression levels in the luminal-like or HER2 breast cancers (Fig. 5). Moreover, AnxA1 gene expression was significantly higher in basal-like than in the other tumor subtypes in the poor prognosis gene signature of van de Vijver et al. (19) ($P <$ 0.001; Table S6), and AnxA1 was found to be overexpressed in two gene signatures described to distinguish BLBC from other subtypes (7, 34). Therefore, we propose AnxA1 as an additional marker to improve diagnostics to better discriminate BLBCs from other subtypes in the clinic. Currently, we are collecting patient material and data for a larger cohort study performed by several independent pathologists (in total >2,000 patients), which will validate the potential of AnxA1 as an official marker for improved identification of the highly aggressive BLBC subtype and its association with a poor prognosis.

Taken together, our data show that AnxA1 is functionally involved in BLBC progression and metastasis formation and is able to regulate TGFβ signaling and actin cytoskeletal reorganization. We propose AnxA1 as an additional marker to improve diagnostics to better discriminate BLBCs from other subtypes in the clinic.

## Materials and Methods

**Cell Line Maintenance and Treatments.** The breast cancer cell lines used for real-time PCR analysis in this study were cultured and characterized for morphology (e.g., epithelial vs. mesenchymal) and E-cadherin promoter methylation as described (11). MTLn3 rat mammary adenocarcinoma cells (35) were cultured as described (36). The 4T1 mouse breast cancer cell line was obtained from American Type Culture Collection (CRL-2539) and cultured in RPMI 1640 Medium (Gibco) supplemented with 10% FBS.

**RNA Isolation and Real-Time PCR.** Cell culture of the panel of breast cancer cell lines described in Fig. 1A, RNA isolation, and RT-PCR was performed as described (11).

**Expression and Knockdown of AnxA1.** For preparation of stable shRNA cell lines, 4T1, MDA-MB-231, and BT549 cells were transduced by using lenti-viral shRNA vectors [Sigma-Aldrich, kindly provided by Rob Hoeben, Leiden University Medical Center (LUMC)]. See *SI Materials and Methods* for sequences. Cells were selected by using puromycin. For transient knockdown of AnxA1 Dharmacon Smartpool siRNAs against GFP (control) or AnxA1 (rat and human) were used. Transfections were performed according to the manufacturer's protocol by using Dharmafect reagent 2 (MTLn3) and 4 (MDA-MB-231, HBL-100) (Dharmacon).

**In Vivo Tumor Growth and Metastasis Formation.** Tumor cells ($1 \times 10^5$ 4T1) in 0.1 mL of PBS were injected into the fat pad of 12-week old female Rag2$^{-/-}$/γc$^{-/-}$ or BALB/c mice. Size of the primary tumors was measured by using calipers. Horizontal ($h$) and vertical ($v$) diameters were determined and tumor volume ($V$) was calculated: $V = 4/3\pi\{1/2[\sqrt{(h \times v)}]^3\}$. Surface lung metastases were counted for each animal using ink injected lungs ($n$ = 5–7 per group). See *SI Materials and Methods* for details on breeding and procedures. All animal experiments were approved by the local ethical committee.

**Antibodies.** See *SI Materials and Methods*.

**Immunohistochemistry.** Tumors and lungs were embedded in paraffin and sectioned (4 μm) onto 3-aminopropyltriethoxysilane-coated slides. After deparaffinization, the tumor and lung sections were stained for H&E and lungs were examined for lung metastasis formation. Paraffin sections were deparaffinized, followed by antigen retrieval in citrate buffer, incubation with primary (phosphoSer465/467-Smad2 or Smad4) and biotynilated secondary antibodies, and a short incubation with Nova-Red. The sections were counterstained with hematoxylin.

**Western Blot Analysis.** Cells were harvested as described (37). See *SI Materials and Methods* for details on antibodies.

**Immunofluorescence and Image Analysis.** Immunofluorescence was performed as described (37). See *SI Materials and Methods* for details on antibodies.

**Luciferase Assays.** Cells cultured in 48-well plates were transfected with (CAGA)$_{12}$-transcriptional luciferase (38) and renilla reporter constructs by using Lipofectamine Plus reagent (Invitrogen). The following day, cells were serum-starved and exposed to TGFβ1 (24 h); thereafter, cells were lysed and luciferase activity was measured by using the dual-luciferase reporter assay system (Promega).

**Patient Selection and Study Design.** Schmidt et al. (39) conducted a retrospective cohort study of breast cancer patients. This cohort includes women who received surgery for invasive breast cancer in LUMC and two regional hospitals in Leiden between 1970 and 1995 (40). The study received approval of the Medical Ethical Committee of the LUMC. The TMA represented 518 cases of breast carcinoma; 66 cases were not analyzed for technical reasons.

**TMA.** Tumor characteristics were all derived from a review of slides stained with H&E and from TMAs including three punches per tumor. Tumor grading, according to the Bloom-Richardson method (41) and tumor morphology typing, was performed as described (39). Immunohistochemical staining of the tissue arrays for AnxA1 was performed at the Pathology Department of the LUMC according to the protocol described in Baelde et al. (42). Evaluation of AnxA1, AnxA2, Src, CK5, and CK8 expression levels was performed independently by two scientists and a pathologist (M.H.v.M., M.d.G., and V.T.S.). The intensity of the staining was scored on a 0–3 scale. Evaluation of ER, PR, p53, and Her2 was performed as described (39). Only those breast carcinomas where staining for all of the eight immunohistochemical markers was successful ($n$ = 295) were included for hierarchical unsupervised cluster analysis (UPGMA method; assuming Euclidian distances between scores) by using the GEPAS package.

**Statistical Analysis in Vitro and in Vivo.** TMA statistical analysis was done by using Statistical Package for the Social Sciences SPSS 15.0 and differences in proportions were tested by Pearson $\chi^2$. For in vitro and in vivo animal studies, Student's $t$ test was used to determine whether there was a significant difference between two means ($P < 0.05$). When multiple means were compared, significance was determined by one-way analysis of variance (ANOVA; $P < 0.05$). Significant differences are marked in the graphs.

1. Lim LH, Pervaiz S (2007) Annexin 1: The new face of an old molecule. *FASEB J* 21: 968–975.
2. de Graauw M, et al. (2008) Annexin A2 phosphorylation mediates cell scattering and branching morphogenesis via cofilin activation. *Mol Cell Biol* 28:1029–1040.
3. Fidler IJ (2003) The pathogenesis of cancer metastasis: The 'seed and soil' hypothesis revisited. *Nat Rev Cancer* 3:453–458.
4. Ahn SH, Sawada H, Ro JY, Nicolson GL (1997) Differential expression of annexin I in human mammary ductal epithelial cells in normal and benign and malignant breast tissues. *Clin Exp Metastasis* 15:151–156.
5. Bai XF, et al. (2004) Overexpression of annexin 1 in pancreatic cancer and its clinical significance. *World J Gastroenterol* 10:1466–1470.
6. Garcia Pedrero JM, et al. (2004) Annexin A1 down-regulation in head and neck cancer is associated with epithelial differentiation status. *Am J Pathol* 164:73–79.
7. Sørlie T, et al. (2001) Gene expression patterns of breast carcinomas distinguish tumor subclasses with clinical implications. *Proc Natl Acad Sci USA* 98:10869–10874.
8. Sorlie T, et al. (2003) Repeated observation of breast tumor subtypes in independent gene expression data sets. *Proc Natl Acad Sci USA* 100:8418–8423.
9. Rouzier R, et al. (2005) Breast cancer molecular subtypes respond differently to preoperative chemotherapy. *Clin Cancer Res* 11:5678–5685.
10. Sarrió D, et al. (2008) Epithelial-mesenchymal transition in breast cancer relates to the basal-like phenotype. *Cancer Res* 68:989–997.
11. Lombaerts M, et al. (2006) E-cadherin transcriptional downregulation by promoter methylation but not mutation is related to epithelial-to-mesenchymal transition in breast cancer cell lines. *Br J Cancer* 94:661–671.
12. Neve RM, et al. (2006) A collection of breast cancer cell lines for the study of functionally distinct cancer subtypes. *Cancer Cell* 10:515–527.
13. Blick T, et al. (2008) Epithelial mesenchymal transition traits in human breast cancer cell lines. *Clin Exp Metastasis* 25:629–642.
14. Polyak K, Weinberg RA (2009) Transitions between epithelial and mesenchymal states: Acquisition of malignant and stem cell traits. *Nat Rev Cancer* 9:265–273.
15. Laping NJ, et al. (2002) Inhibition of transforming growth factor (TGF)-beta1-induced extracellular matrix with a novel inhibitor of the TGF-beta type I receptor kinase activity: SB-431542. *Mol Pharmacol* 62:58–64.
16. Lelekakis M, et al. (1999) A novel orthotopic model of breast cancer metastasis to bone. *Clin Exp Metastasis* 17:163–170.
17. Nielsen TO, et al. (2004) Immunohistochemical and clinical characterization of the basal-like subtype of invasive breast carcinoma. *Clin Cancer Res* 10:5367–5374.
18. Rakha EA, et al. (2007) Breast carcinoma with basal differentiation: A proposal for pathology definition based on basal cytokeratin expression. *Histopathology* 50: 434–438.
19. van de Vijver MJ, et al. (2002) A gene-expression signature as a predictor of survival in breast cancer. *N Engl J Med* 347:1999–2009.
20. Deckers M, et al. (2006) The tumor suppressor Smad4 is required for transforming growth factor beta-induced epithelial to mesenchymal transition and bone metastasis of breast cancer cells. *Cancer Res* 66:2202–2209.
21. Padua D, et al. (2008) TGFbeta primes breast tumors for lung metastasis seeding through angiopoietin-like 4. *Cell* 133:66–77.
22. Tan AR, Alexe G, Reiss M (2008) Transforming growth factor-beta signaling: emerging stem cell target in metastatic breast cancer? *Breast Cancer Res Treat* 115:453–495.
23. Futter CE, White IJ (2007) Annexins and endocytosis. *Traffic* 8:951–958.
24. Goebeler V, Poeter M, Zeuschner D, Gerke V, Rescher U (2008) Annexin A8 regulates late endosome organization and function. *Mol Biol Cell* 19:5267–5278.
25. Morel E, Gruenberg J (2007) The p11/S100A10 light chain of annexin A2 is dispensable for annexin A2 association to endosomes and functions in endosomal transport. *PLoS One* 2:e1118.
26. Morel E, Gruenberg J (2009) Annexin A2 binding to endosomes and functions in endosomal transport are regulated by tyrosine 23 phosphorylation. *J Biol Chem* 284: 1604–1611.
27. Morel E, Parton RG, Gruenberg J (2009) Annexin A2-dependent polymerization of actin mediates endosome biogenesis. *Dev Cell* 16:445–457.
28. Seemann J, Weber K, Osborn M, Parton RG, Gerke V (1996) The association of annexin I with early endosomes is regulated by Ca2+ and requires an intact N-terminal domain. *Mol Biol Cell* 7:1359–1374.
29. Chen YG (2009) Endocytic regulation of TGF-beta signaling. *Cell Res* 19:58–70.
30. Hayes S, Chawla A, Corvera S (2002) TGF beta receptor internalization into EEA1-enriched early endosomes: Role in signaling to Smad2. *J Cell Biol* 158:1239–1249.
31. Penheiter SG, et al. (2002) Internalization-dependent and -independent requirements for transforming growth factor beta receptor signaling via the Smad pathway. *Mol Cell Biol* 22:4750–4759.
32. Hayes MJ, Rescher U, Gerke V, Moss SE (2004) Annexin-actin interactions. *Traffic* 5: 571–576.
33. Nagle RB, et al. (1986) Characterization of breast carcinomas by two monoclonal antibodies distinguishing myoepithelial from luminal epithelial cells. *J Histochem Cytochem* 34:869–881.
34. Charafe-Jauffret E, et al. (2006) Gene expression profiling of breast cell lines identifies potential new basal markers. *Oncogene* 25:2273–2284.
35. Neri A, Welch D, Kawaguchi T, Nicolson GL (1982) Development and biologic properties of malignant cell sublines and clones of a spontaneously metastasizing rat mammary adenocarcinoma. *J Natl Cancer Inst* 68:507–517.
36. Huigsloot M, Tijdens IB, Mulder GJ, van de Water B (2002) Differential regulation of doxorubicin-induced mitochondrial dysfunction and apoptosis by Bcl-2 in mammary adenocarcinoma (MTLn3) cells. *J Biol Chem* 277:35869–35879.
37. de Graauw M, et al. (2005) Heat shock protein 27 is the major differentially phosphorylated protein involved in renal epithelial cellular stress response and controls focal adhesion organization and apoptosis. *J Biol Chem* 280:29885–29898.
38. Dennler S, et al. (1998) Direct binding of Smad3 and Smad4 to critical TGF beta-inducible elements in the promoter of human plasminogen activator inhibitor-type 1 gene. *EMBO J* 17:3091–3100.
39. Schmidt MK, et al. (2007) Breast cancer survival and tumor characteristics in premenopausal women carrying the CHEK2*1100delC germline mutation. *J Clin Oncol* 25:64–69.
40. Schmidt MK, Vermeulen E, Tollenaar RAEM, Van't Veer LJ, van Leeuwen FE (2009) Regulatory aspects of genetic research with residual human tissue: Effective and efficient data coding. *Eur J Cancer* 45:2376–2382.
41. Elston CW, Ellis IO (2002) Pathological prognostic factors in breast cancer. I. The value of histological grade in breast cancer: experience from a large study with long-term follow-up. *Histopathology* 41:151.
42. Baelde HJ, et al. (2007) Reduction of VEGF-A and CTGF expression in diabetic nephropathy is associated with podocyte loss. *Kidney Int* 71:637–645.

**CELL BIOLOGY**